

# Three-Phase 4-Wire Isolated Wind Energy Conversion System Employing VSC with a T-Connected Transformer for Neutral Current Compensation

**Gaurav Kumar Kasal\*** and **Bhim Singh\***

**Abstract** – This paper presents a voltage and frequency controller (VFC) for a 4-wire stand-alone wind energy conversion system (WECS) employing an asynchronous generator. The proposed VF controller consists of a three leg IGBT (Insulated Gate Bipolar Junction Transistor) based voltage source converter and a battery at its DC bus. The neutral terminal for the consumer loads is created using a T-connected transformer, which consists of only two single phase transformers. The control algorithm of the VF controller is developed for the bidirectional flow capability of the active power and reactive power control by which it controls the WECS voltage and frequency under different dynamic conditions, such as varying consumer loads and varying wind speeds. The WECS is modeled and simulated in MATLAB using Simulink and PSB toolboxes. Extensive results are presented to demonstrate the capability of the VF controller as a harmonic eliminator, a load balancer, a neutral current compensator as well as a voltage and frequency controller.

**Keywords:** Stand-alone wind energy conversion system, Voltage source converter, Voltage and frequency control, T-connected transformer, Asynchronous generator

## 1. Introduction

Asynchronous squirrel cage generators (AGs) with their low maintenance and simplified controls appear to be the effective solution for isolated hydro and wind power applications [1-4] where grid supply is not accessible and areas are rich in renewable energy sources. In different stand-alone power applications there are a number of low cost schemes available to control the voltage and frequency of IAGs (isolated asynchronous generators) [5-8]. Substantial work has also been done on the investigation of voltage and frequency (VF) controllers in a stand-alone wind power generating system employing various types of electrical generators [8-14]. However, in grid connected wind power conversion, the frequency remains constant due to the availability of the grid but it's a great challenge in an isolated mode of operation under conditions of varying wind speeds and consumer loads. After careful review of existing literature, it is observed that previously reported work has been concentrated only towards 3-phase 3-wire, or single-phase power conversion using IAGs [5-7]. However, in this work a cost effective VF controller is proposed for a stand-alone 3-phase 4-wire wind power conversion system [15-16].

The main challenge facing a squirrel cage asynchronous generator based isolated wind energy conversion system (WECS) is related to its voltage and frequency controls. Therefore, the need for a voltage and frequency

controller for such isolated systems is mandatory to ensure the satisfactory operation of a WECS. However, due to tremendous advancements in power electronic devices [15] substantial work has also been reported in this area.

In this paper, a voltage and frequency (VF) controller is proposed which consists of a three leg IGBT based voltage source converter (VSC) with a battery [16-19] at its DC bus. The path for the flow of the load neutral current is provided using a T-connected transformer [20] which consists of only two single- phase transformers. However, previously proposed solutions for neutral current compensation are based on the zigzag transformer [21] and the star-delta connected transformer [22]. VSCs with batteries that have bidirectional flow capability for both active and reactive power control the magnitude and frequency of the generated voltage to ensure a constant value. In addition to this, it also functions as a harmonic eliminator, a load balancer and a load leveler [23, 24].

## 2. System Configuration

Fig. 1 shows the proposed isolated wind energy conversion system (WECS) along with a new voltage and frequency controller. This WEC system consists of a wind turbine driven asynchronous generator and its VF controller, is connected at the point of common coupling. Three legs of the VSC are connected to the three phases through interfacing inductors. The T-connected transformer is connected in parallel branch of the VSC based controller to provide a neutral terminal for the loads. The transformer acts as a path for zero-sequence components of load cur-

\* Dept. of Electrical and Electronic Engineering, Indian Institute of Technology New Delhi, India  
(gauravkasal@gmail.com, bsingh@ee.iitd.ac.in)

Received 19 August 2008; Accepted 10 February 2009

rents while the VSC and battery are there for the purpose of harmonic elimination, load balancing, load leveling and reactive power compensation. The T-connected transformer is regarded as an open-circuit for positive and negative sequence currents so that the current at the generator terminal remains balanced.

### 3. Control Strategy

Fig. 2 shows the control scheme of the VSC based VF controller to regulate the magnitude and frequency of voltage at the generator terminals. Three-phase reference source currents consist of two components: one is an in phase or active power component ( $i_{da}^r, i_{db}^r, i_{dc}^r$ ) for regulating frequency, while the other is in quadrature or the reactive power component of the source currents ( $i_{qa}^r, i_{qb}^r, i_{qc}^r$ ) for regulating terminal voltage. The amplitude of the active power component of the source current ( $I_{dm}$ ) is estimated by taking the difference of  $I_{dm1}$  and  $I_{dm2}$ . The value of  $I_{dm1}$  is estimated by dividing the filtered load power ( $P_{Lfilter}$ ) to the amplitude of the terminal voltage ( $V_t$ ) while the  $I_{dm2}$  is the output of the PI (Proportional-Integral) frequency controller. The multiplication of  $I_{dm}$  with in-phase unit amplitude templates ( $u_{ad}, u_{bd}$  and  $u_{cd}$ ) yields the in-phase component of reference source currents ( $i_{da}^r, i_{db}^r, i_{dc}^r$ ). These ( $u_{ad}, u_{bd}$  and  $u_{cd}$ ) templates are three-phase sinusoidal functions and are derived by unit templates of in phase with line voltages ( $u_{ab}, u_{bc}, u_{ca}$ ). The templates ( $u_{ab}, u_{bc}, u_{ca}$ ) are derived by dividing the AC line voltages  $v_{ab}, v_{bc}$  and  $v_{ca}$  by their amplitude  $V_t$ . To generate the quadrature component of reference source currents, another set of sinusoidal quadrature unity amplitude templates ( $u_{aq}, u_{bq}, u_{cq}$ ) is obtained from in-phase unit templates ( $u_{abd}, u_{bcd}, u_{cad}$ ). The multiplication of these components with the output of the PI voltage controller ( $I_{qm}$ ) gives the quadrature, or reactive power component of the reference source currents. The sum of the instantaneous quadrature and in-phase component of source currents is the reference source currents ( $i_{sa}^r, i_{sb}^r$  and  $i_{sc}^r$ ), and each phase current is compared with the corresponding reference current to generate

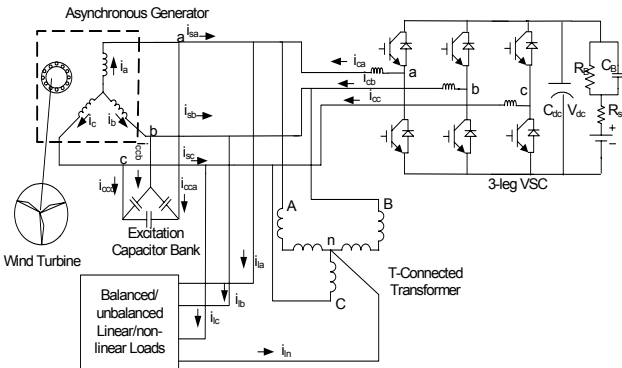


**Fig. 1.** Schematic diagram of a proposed WECS configuration

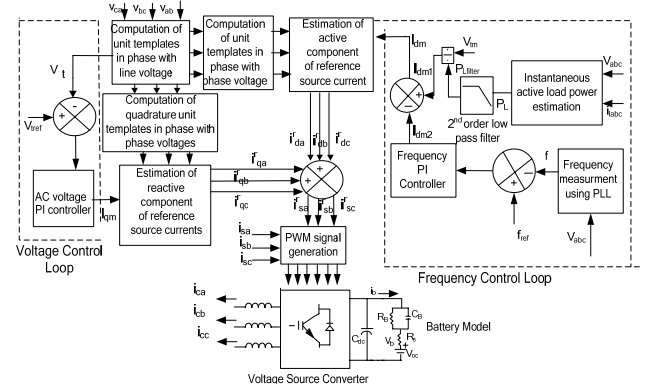


**Fig. 2.** Control scheme of the proposed VF controller for WECS

the PWM switching signal for the VSC of the VF controller. The complete control algorithm of the WECS is explained as follows.

### 4. Control Algorithm

Basic equations of the control scheme of the proposed VF controller are as follows.

#### 4.1 Computation of Active Component of Reference Source Currents

The active component of the reference source current is estimated as follows.

The load power ( $P_L$ ) is estimated by taking a 3-phase to 2-phase transform as:

$$v_\alpha = (\sqrt{2}/3)(1/\sqrt{3})(v_{ab} - \frac{1}{2}v_{bc} - \frac{1}{2}v_{ca}) \quad (1)$$

$$v_\beta = (\sqrt{2}/3)(1/\sqrt{3})(\sqrt{3}/2v_{bc} - \sqrt{3}/2v_{ca}) \quad (2)$$

$$i_\alpha = (\sqrt{2}/3)(i_{la} - \frac{1}{2}i_{lb} - \frac{1}{2}i_{lc}) \quad (3)$$

$$i_\beta = (\sqrt{2}/3)(\sqrt{3}/2i_{lb} - \sqrt{3}/2i_{lc}) \quad (4)$$

Instantaneous active power of the load is estimated as:

$$P_L = v_\alpha i_\alpha + v_\beta i_\beta \quad (5)$$

It is filtered to achieve its DC component ( $P_{Lfilter}$ ), which is an active power of the load.

The  $I_{dm1}$  is calculated as:

$$I_{dm1} = 2(P_{Lfilter})/(3V_t) \quad (6)$$

The frequency error is defined as:

$$f_{er(n)} = f_{ref(n)} - f(n) \quad (7)$$

where “ $f_{ref}$ ” is the reference frequency (50Hz in the present system) and ‘ $f$ ’ is the frequency of the voltage of an asynchronous generator. The instantaneous value of ‘ $f$ ’ is estimated using phase locked loop (PLL) over the terminal voltage of the generator.

At the  $n^{th}$  sampling instant, output of PI frequency controller ( $I_{dm2}$ ) is as:

$$I_{dm2(n)} = I_{dm2(n-1)} + K_{pf}\{f_{er(n)} - f_{er(n-1)}\} + K_{if}f_{er(n)} \quad (8)$$

Therefore amplitude of the active power current component ( $I_{dm}$ ) of the reference source currents is:

$$I_{dm} = I_{dm1} - I_{dm2} \quad (9)$$

The instantaneous line voltages at the terminals of an asynchronous generator ( $v_{ab}, v_{bc}$  and  $v_{ca}$ ) are considered sinusoidal and their amplitude is computed as:

$$V_t = \{(2/3)(v_{ab}^2 + v_{bc}^2 + v_{ca}^2)\}^{1/2} \quad (10)$$

The unity amplitude templates are having instantaneous value in phase with instantaneous line voltages ( $v_{ab}$ ,  $v_{bc}$  and  $v_{ca}$ ), which are derived as:

$$u_{ab} = v_{ab}/V_t; u_{bc} = v_{bc}/V_t; u_{ca} = v_{ca}/V_t \quad (11)$$

From these line voltage templates unit templates the in phase with phase voltage can be estimated using a 30° leading transform as:

$$u_{ad} = (\sqrt{3}/2) u_{ab} + \{1/(2\sqrt{3})\} \{ (u_{bc} - u_{ca}) \} \quad (12)$$

$$u_{bd} = -(\sqrt{3}/2) u_{ab} + \{1/(2\sqrt{3})\} \{ (u_{bc} - u_{ca}) \} \quad (13)$$

$$u_{cd} = -(1/\sqrt{3}) \{ (u_{bc} - u_{ca}) \} \quad (14)$$

The in-phase components of reference source currents are estimated as:

$$i_{da}^r = I_{dm} u_{ad}; i_{db}^r = I_{dm} u_{bd}; i_{dc}^r = I_{dm} u_{cd}; \quad (15)$$

## 4.2 Computation of the Reactive Component of Reference Source Currents

The error in amplitude of AC voltage  $V_{er}$  at the  $n^{th}$  sampling instant as,

$$V_{er(n)} = V_{tref(n)} - V_{t(n)} \quad (16)$$

where  $V_{tref(n)}$  is the amplitude of reference AC terminal voltage and  $V_{t(n)}$  is the amplitude of the sensed three-phase AC voltage at the terminals of an asynchronous generator at  $n^{th}$  instant is computed.

The output of the AC voltage PI controller ( $I_{qm(n)}$ ) for maintaining constant AC terminal voltage at the  $n^{th}$  sampling instant is expressed as:

$$I_{qm(n)} = I_{qm(n-1)} + K_{pa} \{ V_{er(n)} - V_{er(n-1)} \} + K_{ia} V_{er(n)} \quad (17)$$

where  $K_{pa}$  and  $K_{ia}$  are the proportional and integral gain constants of the PI controller (values are given in Appendix).  $V_{er(n)}$  and  $V_{er(n-1)}$  are the voltage errors in  $n^{th}$  and  $(n-1)^{th}$  instants and  $I_{qm(n-1)}$  is the amplitude of quadrature component of the reference source current at  $(n-1)^{th}$  instant.

The instantaneous quadrature components of reference source currents are estimated as:

$$i_{qa}^r = I_{qm} u_{aq}; i_{qb}^r = I_{qm} u_{bq}; i_{qc}^r = I_{qm} u_{cq} \quad (18)$$

where  $u_{aq}$ ,  $u_{bq}$  and  $u_{cq}$  are another set of unit templates having a phase shift of 90° leading the corresponding unit templates  $u_{ad}$ ,  $u_{bd}$  and  $u_{cd}$  which are computed as follows:

$$u_{aq} = (1/2) u_{ab} - \sqrt{3} (u_{bc} - u_{ca}) / (2\sqrt{3}) \quad (19)$$

$$u_{bq} = (1/2) u_{ab} + \sqrt{3} (u_{bc} - u_{ca}) / (2\sqrt{3}) \quad (20)$$

$$u_{cq} = -u_{ab} \quad (21)$$

## 4.3 Computation of Reference Source Currents

The reference source currents are the sum of in-phase and quadrature components of the reference source currents as:

$$i_{sa}^r = i_{qa}^r + i_{da}^r \quad (22)$$

$$i_{sb}^r = i_{qb}^r + i_{db}^r \quad (23)$$

$$i_{sc}^r = i_{qc}^r + i_{dc}^r \quad (24)$$

## 4.4 PWM Signal Generation

Reference source currents ( $i_{sa}^r$ ,  $i_{sb}^r$  and  $i_{sc}^r$ ) are compared with sensed source currents ( $i_{sa}$ ,  $i_{sb}$  and  $i_{sc}$ ). The current errors are computed as:

$$i_{saerr} = i_{sa}^r - i_{sa} \quad (25)$$

$$i_{sberr} = i_{sb}^r - i_{sb} \quad (26)$$

$$i_{scerr} = i_{sc}^r - i_{sc} \quad (27)$$

These current errors are amplified using proportional controller by gain 'K' and which are as follows:

$$V_{cca} = K i_{saerr} \quad (28)$$

$$V_{ccb} = K i_{sberr} \quad (29)$$

$$V_{ccc} = K i_{scerr} \quad (30)$$

These amplified signals are compared with fixed frequency (10 kHz) triangular carrier waves to generate gating signals for the VSC of each phase of the VF controller.

## 5. MATLAB Based Modeling

The proposed VF controller is modeled and simulated in MATLAB using Simulink and PSB (Power System Block set) toolboxes. A 22 kW, 415V, 50Hz asynchronous machine is used as a generator and includes the saturation characteristics of the machine, which is determined by a synchronous speed test [6]. A delta connected excitation capacitor is used to generate the rated voltage at no-load [6], while an additional demand of the generator's reactive power during load variation is met by the proposed VF controller. An in-built universal bridge is used as a three leg voltage source converter and the Thevenin equivalent battery model with parallel is used at it DC bus. The wind turbine modeling is also carried out in MATLAB. All necessary equations to model the control algorithm, such as the calculation of terminal voltage, unit vectors, etc., are carried out using function blocks. Simulation is carried out in MATLAB version 7.1 using an ode (23tb/stiff/TR-BDF-2) solver in discrete mode at 5e-6 step size.

In Fig 1, the battery is represented as an equivalent to the Thevenin model and its charging and discharging depends upon the availability of wind energy and consumer loads. Since the battery is an energy storage unit, its energy is represented in kWh when a capacitor is used to model the battery unit, the capacitance can be determined from

$$C_B = \frac{kWh * 3600 * 10^3}{0.5(V_{ocmax}^2 - V_{ocmin}^2)} \quad (31)$$

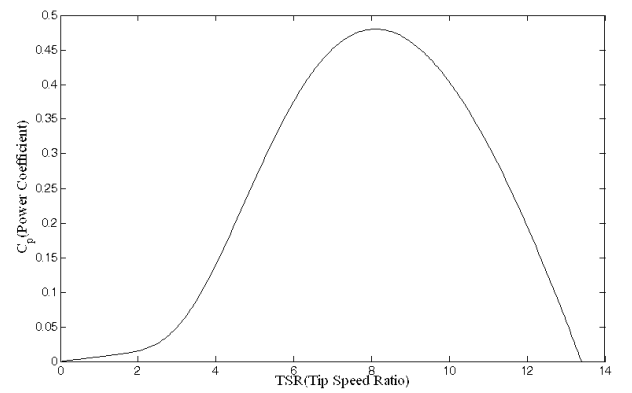


Fig. 3. Curve between power coefficients (Cp) and tip speed ratio ( $\lambda$ )

In the Thevenin equivalent model of the battery,  $R_s$  is the equivalent resistance (external + internal) of the parallel/series combination of a battery, which is usually a small value. The parallel circuit of  $R_B$  and  $C_B$  is used to model the stored energy and voltage during charging or discharging.  $R_B$  in parallel with  $C_B$ , represents the self-discharging of the battery. Since the self-discharging current of a battery is small, the resistance  $R_B$  is large. Here, the battery is considered to have 18 kW for 6 Hrs peaking capacity, and a variation in the voltage in the order of 790V-810V.

Fig. 3 shows the curve between the power coefficient ( $C_p$ ) and tip speed ratio ( $\lambda$ ) at a fixed pitch angle ( $\beta$ ). It shows that  $C_p$  reaches a maximum value (0.48) for a tip speed ratio (8.1), which yields the maximum mechanical power available in the wind turbine for a given wind speed. The tip speed ratio (TSR) is defined as the ratio of the linear speed at the tip of the blade ( $\omega_T R$ ) and the wind speed ( $v_w$ ),  $\omega_T$  being the rotational speed of the wind turbine. The polynomial relation between  $C_p$  and  $\lambda$  at a particular pitch angle for the wind turbine under consideration [1] is represented as

$$C_p = C_1 \{(C_2/\lambda i) - C_3 \beta - C_4\} e^{-(C_5/\lambda i)} + C_6 \lambda \quad (32)$$

where  $1/\lambda i = \{1/(\lambda + C_7 \beta)\} - \{C_8/(\beta^3 + 1)\}$  and  $\beta = 0^\circ$

## 6. Results and Discussion

Figs. 4-7 show the performance of the proposed stand-alone wind generating system under the dynamic conditions of varying loads and varying wind speeds. Different transient waveforms of the generator are shown in Figs 4-6 to demonstrate the performance of the VF controller for supplying balanced/unbalanced, linear/non-linear respectively. Fig. 7 demonstrates the performance of the VF controller under conditions of varying wind speed, and it is observed that in all conditions the VF controller responds in a desirable manner. Simulated transient waveforms of the generator voltage with respect to neutral ( $v_{abcn}$ ), generator current ( $i_{abc}$ ), capacitor current ( $i_{cca}$ ), load currents ( $i_{labc}$ ), load neutral current ( $i_{ln}$ ), controller current ( $i_{cabc}$ ), wind speed ( $v_w$ ), battery current ( $i_b$ ), battery voltage ( $V_b$ ), terminal voltage ( $V_t$ ), frequency ( $f$ ), instantaneous active load power and filtered power ( $P_L$  and  $P_{L\text{filter}}$ ), variation in consumer power ( $P_{\text{load}}$ ), battery power ( $P_{\text{bat}}$ ) and generator power ( $P_{\text{gen}}$ ) and variation in VA rating of the transformer with variation of consumer load ( $T_{VA}$ ) are given in different dynamic conditions.

### 6.1 Performance of the VF Controller Feeding 0.8 pf Lagging Reactive Load

The performance of the controller with balanced/unbalanced 0.8 pf lagging reactive load is demonstrated in Fig. 4 at a wind speed of 8m/s. Three single-phase loads are applied between each phase and neutral at 1.5 sec. At 1.65 sec an opening of one phase occurs, followed by another phase at 1.8 sec, and the load becomes unbalanced. In

both cases it is observed that the voltage and frequency of the system remain constant. At 1.95 sec, the load is fully removed from the WECS and it is observed that the VF controller responds in a desirable manner to regulate the voltage and frequency. Here, the transformer VA rating ( $T_{VA}$ ) is also presented with variation of the load so that one can estimate the rating of the proposed T-connected transformer.

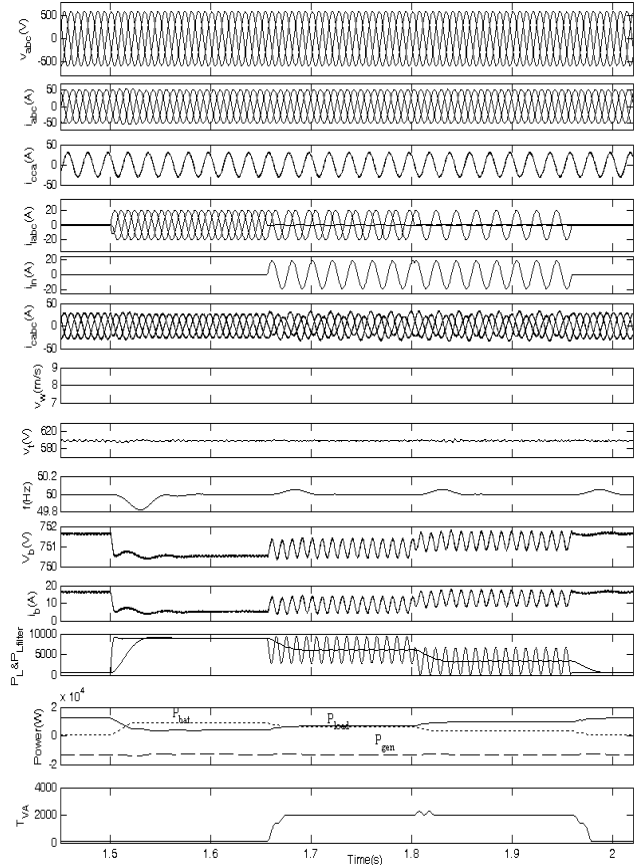


**Fig. 4.** Performance of the VF controller under application of balanced/unbalanced 0.8 pf lagging reactive loads

### 6.2 Performance of the VF Controller Feeding Non-linear Loads

The performance of the controller with balanced/unbalanced non-linear loads is demonstrated in Fig. 5 at a wind speed of 8m/s. Three single-phase diode bridge rectifiers with L-C filter based non-linear loads are applied between each phase and neutral at 1.5 sec. At 1.65 sec an opening of one phase and another phase at 1.8 sec, the load becomes unbalanced. In both cases it is observed that the voltage and frequency of the WEC system remain constant. At 1.95 sec, the load is fully removed from the WECS and it is observed that the VF controller regulates the voltage and frequency, along with the additionally mentioned features of load balancing and harmonic elimination.

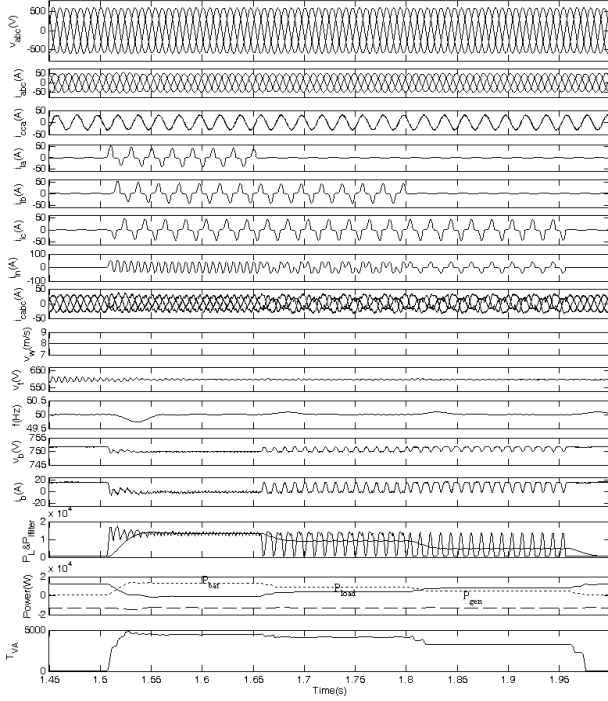


**Fig. 5.** Performance of the VF controller under application of balanced/unbalanced non-linear loads

Table 1 demonstrates the total harmonic distortion (THD) at the generator terminals under non-linear loads. It is observed that the VF controller maintains the THD at the generator voltage and a current of under 5% of the limit imposed by IEEE - 519 standards [24]. In this way, it is demonstrated that the proposed voltage and frequency controller also provides the function of a harmonic eliminator.

### 6.3 Performance of the VF Controller Feeding Mixed Loads

Fig 6 demonstrates the performance of the VF controller while feeding different types of consumer loads simultaneously, such as a single phase induction motor at the first phase, a 0.8 pf lagging single phase reactive load at the second phase, and single phase diode rectifier based non-linear loads on the third phase of the WECS.

At 1.5s, a 1 hp, 220V, 50Hz, 1480rpm capacitor start and capacitor run single phase induction motor is started and it is observed that, due to the sudden direct on line starting of the motor, the generator power ( $P_{gen}$ ) is increased momentarily. However, due to the action of the proposed VF controller, the frequency and voltage are maintained at their reference value.

At 1.7 sec, while an induction motor is running, a 0.8 pf lagging single phase reactive load of 5kW is applied between phase 'b' and the neutral terminal and it is observed that along with load balancing, the VF controller also maintains a constant voltage and frequency at the terminals of generator.

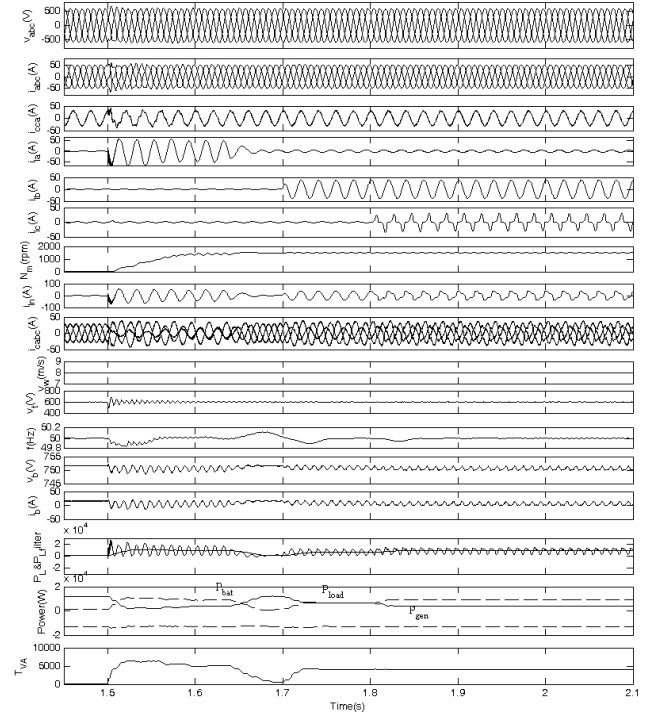


**Fig. 6.** Performance of the VF controller feeding mixed loads (single phase induction motor load, 0.8pf lagging reactive load, single phase non-linear load)

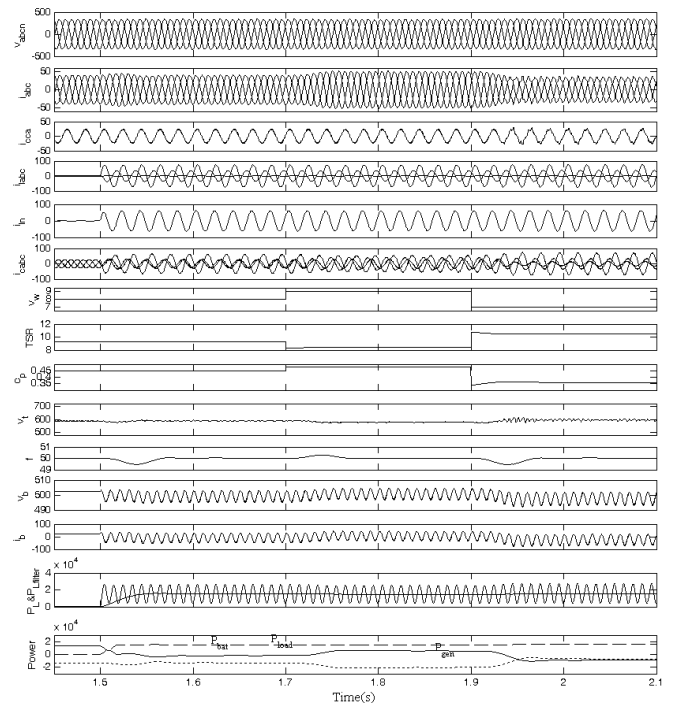


**Fig. 7.** Transient waveforms during variation of wind speed at fixed unbalanced consumer load

At 1.8 sec, between the third phase and the neutral terminal, a single-phase diode rectifier based non-linear load is also applied to the generator. It is observed that in

**Table 1.** Percentage THD OF GENERATOR Voltage, Current, Consumer Load Current At Different Consumer Loads

Non-linear Loads	%THD of generator voltages			%THD of generator currents			% THD of consumer load currents		
	$v_a$	$v_b$	$v_c$	$i_a$	$i_b$	$i_c$	$i_{la}$	$i_{lb}$	$i_{lc}$
Balanced full load (12kW)	.96	.22	.95	2.18	2.27	2.3	48	45.6	45.2
Unbalanced two phase load (8kW)	1.14	1.15	1.08	2.24	2.44	2.4	-	48.5	48.8

all such load conditions, the VF controller responds in a desirable manner and maintains constant voltage and frequency values while functioning as a load balancer and a harmonic eliminator.

#### 6.4 Performance of the VF Controller Under Varying Wind Speed Conditions

Fig. 7 demonstrates the performance of the VF controller under varying wind speed conditions and unbalanced fixed consumer loads. At 1.5 sec, when the wind speed is 8m/s, an unbalanced consumer load of 18kW 0.8 pf lagging reactive load is applied to the WECS. It is observed that due to insufficient power generation at a low wind speed, additional power required by the load is supplied from the battery to regulate the frequency. At 1.7, sec as the wind speed is increased from 8m/s to 9m/s, the output power of the generator ( $P_{gen}$ ) is increased at a particular load now the power supplied by the battery ( $P_{bat}$ ) is reduced and it starts charging as the load demand is now met by the generator itself due to and the availability of ample wind power. At 1.9 sec, the wind speed is reduced from 9m/s to 7m/sec and it is observed that the battery again starts discharging in order to meet the consumer load demand. In this manner, the controller provides load leveling and regulation of the frequency of the WECS.

### 7. Conclusion

The performance of the proposed voltage and frequency controller has been demonstrated for an isolated wind energy conversion system feeding linear, non-linear and dynamic loads under varying wind speed conditions. The proposed T-connected transformer has facilitated the path for the flow of load neutral current. The proposed WECS configuration is simple and requires fewer transformers. It is observed that the VF controller regulates the system voltage and frequency under varying electrical dynamic (varying consumer load) conditions as well as varying mechanical dynamic (varying wind speed) conditions.

### 8. Appendix

#### 8.1 Parameters of 22kW, 415V, 50Hz, Y-Connected, 4-Pole Asynchronous Machine

$$R_s = 0.2511\Omega, R_r = 0.2489\Omega, X_{lr} = X_{ls} = .52\Omega, J = 0.304 \text{ kg-m}^2, C = 12 \text{ kVAR}$$

$$\begin{aligned} L_m &= 0.075 & I_m < 8.0 \\ L_m &= 0.075 - 0.003(I_m - 8.0) & 8 < I_m < 13 \\ L_m &= 0.06 - 0.002(I_m - 13) & 13 < I_m < 23 \\ L_m &= 0.041 & I_m > 23 \end{aligned}$$

#### 8.2 Voltage Rating of the T-Connected Transformer

If one considers voltage across each phase and neutral is 'v' volts, then the voltage across both sides of the T configuration is:

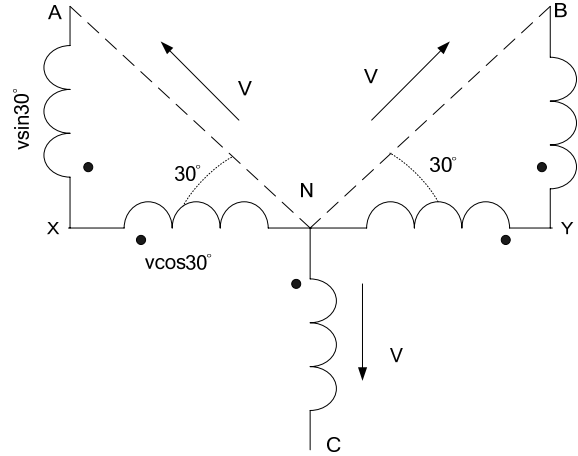
$$V_{NY} = V_{NX} = V \cos 30^\circ = 0.866V$$

$$V_{BY} = V_{AX} = V \sin 30^\circ = 0.5V$$

Therefore, for  $V = 240V$ , the voltage across all other windings can be determined by above equations:

$$V_{NY} = V_{NX} = 207V$$

$$V_{BY} = V_{AX} = 120V$$



#### 8.3 Controller Parameters

Frequency PI Controller  $K_{pf} = 3$ ,  $K_{if} = 150$

AC Voltage PI Controller  $K_{pa} = 0.03$ ,  $K_{ia} = 0.002$

#### 8.4 Wind Turbine Specification

Rating 22kW,  $C_{pmax} = .48$ ,  $\lambda_m = 8.1$ ,  
 $C_1 = 0.5176$ ,  $C_2 = 116$ ,  $C_3 = 0.4$ ,  $C_4 = 5$ ,  $C_5 = 21$ ,  
 $C_6 = 0.0068$ ,  $C_7 = 0.08$ ,  $C_8 = 0.035$ .

## References

- [1] Heier, Siegfried, “*Grid Integration of Wind Energy Conversion Systems*”, John Wiley & Sons Ltd., Chichester, UK, 1998.
- [2] Godoy Simoes, M., and Farret, Felix A., “*Alternative Energy Systems*,” CRC Press Florida, 2008.
- [3] Boldea, Ion, “*Variable Speed Generators*”, CRC Press, Florida 2006.
- [4] Lai, L.L., and Chan, T.F., “*Distributed Generation-Induction and Permanent Magnet Generators*”, John Wiley and Sons Ltd., Chichester, UK, 2007.
- [5] Chen, Woei-Luen, Lin, Yung-Hsiang, Gau, Hrong-Sheng, and Yu, Chia-Hung, “STATCOM controls for a self-excited induction generator feeding random loads”, *IEEE Transactions on Power Delivery*, , vol. 23, no. 4, pp 22-07-2215, Oct 2008.
- [6] Singh, Bhim, Murthy, S.S., and Gupta, Sushma, “STATCOM based voltage regulator for self excited induction generator feeding non-linear loads”, *IEEE Trans. on Industrial Electronics*, vol. 53, no. 5, pp 1437-1452, Oct 2006.
- [7] Marra, G., and Pomilo, J. A., “Induction-generator-based system providing regulated voltage with constant frequency”, *IEEE Trans. on Industrial Electronics*, vol.47, no. 4, pp. 908-914, Aug 2000.
- [8] Lopes, Luiz A.C., and Almeida, Rogerio G., “Wind-driven self excited induction generator with voltage and frequency regulated by a reduced rating voltage source inverter”, *IEEE Trans on Energy Conversion*, vol .21, no. 2, pp 297-304, June 2006.
- [9] Joshi, Dheeraj, Sandhu, K.S., and Soni, M.K., “Constant voltage constant frequency operation for a self-excited induction generator”, *IEEE Transactions on Energy Conversion*, vol. 21, no. 1, pp 228-234, March 2006.
- [10] Singh, Bhim, and Kasal, Gaurav Kumar, “Voltage and frequency controller for a 3-phase 4-wire autonomous wind energy conversion system”, *IEEE Trans. on Energy Conversion*, vol. 23, no. 2, pp 509-518, June 2008.
- [11] Singh, Bhim, and Kasal, Gaurav Kumar, “Solid state voltage and frequency controller for a stand-alone wind power generating system”, in *IEEE Trans on Power Electronics*, vol. 23, no. 3, pp 1170-1177, May 2008.
- [12] Jain, Amit Kumar, and Ranganathan, V. T., “Wound rotor induction generator with sensor-less control and integrated active filter for feeding nonlinear loads in a stand-alone grid”, *IEEE Transactions on Industrial Electronics*, vol. 55, no. 1, pp 218-228, Jan 2008.
- [13] Nayar, C.V., Perahia, J., Thomas, F., Phillips, S. J., Pryor, T., and James, W. L., “Investigation of capacitor excited induction generators and permanent magnets alternators for small scale wind power generation”, *Renewable Energy*, vol. 1, no ¾, pp 381-388, July 1991.
- [14] Shaltout, A. A., and Abdel-Halim, M. A., “Solid state control of wind driven self-excited induction generator”, *Electric Machines and Power Systems*, vol. 23, no. 5, pp 571-582, Sept-Oct 1995.
- [15] Carrasco, Juan Manuel, Franquelo, Leopoldo Garcia, Bialasiewicz, Jan T., Galván, Eduardo, Member, IEEE, Guisado, Ramón C. Portillo, Prats, Ma. Ángeles Martín, León, José Ignacio, and Moreno-Alfonso, Narciso, “Power-Electronic Systems for the Grid Integration of Renewable Energy Sources: A Survey”, *IEEE Transactions on Industrial Electronics*, vol. 53, no. 4, pp 1002-1016, Aug 2006.
- [16] Monteror, Maria Isabel Milanes, Codaval, Enri- que Romero, and Gonzalez, Fermín Barrero, “Comparison of control strategies for shunt active power filters in three-phase four-wire systems”, *IEEE Trans on Power Electronics*, vol. 22, no.1, pp 229-236, Jan 2007.
- [17] Barrado, J.A., and Grino, R., “Voltage and frequency control for a self excited induction generator using a 3-phase 4-wire electronic converters”, in *Proc of 12th International IEEE Power Electronics and Motion Control Conference*, Aug 2006, pp 1419-1424.
- [18] Aderson, M.D., and Carr, D.S., “Battery energy storage technology”, *IEEE Proc*, vol. 81, pp 475-479, March 1993.
- [19] Barton, John P., and Infield, David G., “Energy storage and its use with intermittent renewable energy”, *IEEE Transactions on Energy Conversion*, vol. 19, no. 2, pp 441-448, June 2004.
- [20] Singh, Bhim, Garg, Vipin, and Bhuvaneswari, G., “A novel T-connected autotransformer-based 18-pulse AC-DC converter for harmonic mitigation in adjustable-speed induction-motor drives”, *IEEE Transactions on Industrial Electronics*, vol. 54, no. 5, pp 2500-2511, Oct 2007.
- [21] Choi, Sewan, and Jang, Minsoo, “Analysis and control of a single-phase-inverter-Zigzag-transformer hybrid neutral-current suppressor in three-phase four-wire systems”, *IEEE Transactions on Industrial Electronics*, vol. 54, no. 4, pp 2201-2208, Aug 2007.
- [22] Enjeti, P.N., Shireen, Wajihah, Packebush, Paul, and Pitel, Ira J., “Analysis and design of a new active power filter to cancel neutral current harmonics in three-phase four-Wire electric distribution systems”, *IEEE Transactions on Industry Applications*, vol. 30, no. 6, pp 1565-1572, Dec 1994.
- [23] Akagi, H., Watanabe, E. D., and Aredes, M.M., “*Instantaneous Power Theory and Applications to Power Conditioning*”, John Willey and Sons Ltd., Hoboken, NJ, 2007.
- [24] IEEE Guide for Harmonic Control and Reactive Compensation of Static Power Converters, IEEE Standard 519-1992.



**Gaurav Kumar Kasal** was born in Bhopal, India, in Nov., 1978. He received his B.E. (Electrical) and M.Tech. degrees from the National Institute of Technology (NIT) Allahabad and National Institute of Technology (NIT) Bhopal, India, respectively, in 2002 and 2004. Since Dec. 2004, he

has been pursuing his Ph.D. with the Department of Electrical Engineering at the Indian Institute of Technology (IIT) in Delhi, New Delhi, India, and is currently working as a senior engineer (R&D) in Delta energy systems (India). His field of interest includes power electronics and he has published papers in 21 international journals and 23 international conferences including 1 Indian patent.



**Bhim Singh** was born in Rahamapur, India, in 1956. He received his B.E. (Electrical) degree from the University of Roorkee, Roorkee, India, in 1977 and his M.Tech. and Ph.D. degrees from the Indian Institute of Technology (IIT) Delhi, New Delhi, India, in 1979 and 1983, respectively. In 1983,

he joined the Department of Electrical Engineering, University of Roorkee, as a Lecturer, and in 1988 became a Reader. In December 1990 he joined the Department of Electrical Engineering, IIT Delhi, as an Assistant Professor. He became an Associate Professor in 1994 and Professor in 1997. His area of interest includes power electronics, electrical machines and drives, active filters, and analysis and digital control of electrical machines.

Dr. Singh is a fellow of the Indian National Academy of Engineering (INAE), the Institution of Engineers (India) (IE(1)), and the Institution of Electronics and Telecommunication Engineers (IETE), a life member of the Indian Society for Technical Education (ISTE), the System Society of India (SSI), and the National Institution of Quality and Reliability (NIQR) and a Senior Member of the Institute of Electrical and Electronics Engineers (IEEE).